

Calorimetric study on the influence of calcium sulfate on the hydration of Portland cement–calcium aluminate cement mixtures

Linglin Xu · Peiming Wang · Guofang Zhang

Received: 12 July 2011 / Accepted: 13 September 2011 / Published online: 5 October 2011
© Akadémiai Kiadó, Budapest, Hungary 2011

Abstract The influence of calcium sulfate with different reactivities (anhydrite, α -hemihydrate, and gypsum) on the Portland cement–calcium aluminate cement (PC/CAC) mixtures was presented in the paper. The hydration process and main hydration products (ettringite) of the binders with different content of calcium sulfate was investigated by isothermal conduction calorimetry, setting times, compressive strength, X-ray diffraction (XRD) analysis, and environmental scanning electronic microscope (ESEM) analysis. It is found that the pure PC/CAC mixture without any calcium sulfate addition exhibits very slow hydration kinetics during the first 2 days. By adding calcium sulfate, the setting of the PC/CAC mixture is delayed, but the hydration can be accelerated. The results also show that the reactivity and the amount of the calcium sulfate determine the balance between the hydration products of ettringite and monosulphoaluminate, and also the early hydration kinetics not only in the formation content but in the location of ettringite. In general, when a high content of reactive α -hemihydrate is added, much secondary gypsum forms in voids between cement granules which exert adverse effects on the properties of PC/CAC mixtures. Additionally, ettringite can be formed stably and good binders having good physical properties can be obtained when low reactive anhydrite is added.

Keywords Calcium aluminate cement · Calorimetry · Hydration · Calcium sulfate · Ettringite

Introduction

Calcium aluminate cement (CAC) is known as an indispensable material in the construction field for its resistance to chemical attack and high temperatures [1]. In the dry-mix mortar industry, such as self-leveling screeds, tile adhesives, grouting mortars and rapid-hardening repair mortars, CAC is an essential part of the hydraulic binder. Additionally, it is well known that CAC is added into Portland cement (PC) to accelerate setting [2–5]. But, the replacement of PC with CAC has been found to result in a great decrease of compressive strength especially at later age [2, 6, 7], which becomes a barrier for the application of PC/CAC mixtures. It may result from the film-like hydration products that surround anhydrate granules at early age [2, 3], which significantly delay later hydration of PC/CAC mixtures. Therefore, it is of prime importance to improve the strength of PC/CAC mixtures to obtain full benefits of CAC to dry-mix mortar industry. There are several ways to improve later strength, for instance, adding mineral additives [8, 9] or chemical additives [10, 11]. Especially, calcium sulfate (in the forms of gypsum, anhydrite, or hemihydrate) is mostly used for its economy among those additives.

Many researchers reported the ternary binder system (ternary system) which contains PC, CAC, and calcium sulfate is widely applied in dry-mix mortars [12–18]. The hydration of the ternary system is a complex process since every material has its own reactions which are, however, affected by each other. According to Amathieu et al. [3] and Kighelman et al. [19], ettringite is the main phase

L. Xu · P. Wang (✉) · G. Zhang
School of Materials Science and Engineering, Tongji University,
Shanghai 201804, China
e-mail: tjwpm@126.com

L. Xu
e-mail: xulinglinok@hotmail.com

P. Wang · G. Zhang
Key Laboratory of Advanced Civil Engineering Materials,
Ministry of Education, Shanghai 201804, China

Table 1 Chemical composition of raw materials (wt%)

	SiO ₂	CaO	Al ₂ O ₃	Fe ₂ O ₃	MgO	SO ₃	K ₂ O	Na ₂ O	TiO ₂	Loss
PC	21.50	65.20	4.14	2.40	2.57	2.89	0.84	0.67	0.32	2.67
CAC	0.34	31.20	67.10	0.10		0.06	–	0.34	–	–
A	1.72	39.44	0.35	0.16	1.80	51.96	–	–	0.02	4.41
G	18.13	24.50	5.29	1.96	3.17	29.80	–	–	–	–
H	2.05	40.30	0.08	0.02	0.01	57.30	–	–	–	–

formed in such ternary system. Synchrotron X-ray diffraction also indicates that ettringite crystallizes immediately after wetting PC [20]. The formation of ettringite controls the setting rate of the highly reactive aluminate phases [5], such as tricalcium aluminate (C₃A) in PC and monocalcium aluminate (CA) in CAC which react with calcium sulfate, so it is of great importance for the relevant properties like rapid hardening, high strength [18] and expansive proportion [21]. Thus, the investigation on the formation of ettringite during the early age is one of the key issues.

Previous investigations have demonstrated that a certain form of calcium sulfate shows a particular solubility and rate of dissolution [22–24], as a consequence, the sources and content of calcium sulfate used, dominate the formation time and content of ettringite [25–27]. Although lots of studies have focused on the performance of the ternary system; no work has dealt with the influence of different sources and contents of calcium sulfate on the hydration process in PC/CAC mixtures.

The calorimetric measurement is a well-established method to study the kinetics and mechanism of hydration in cementitious materials in situ [28] since it shows great versatility in studying the hydration kinetics of cementitious systems and help to monitor cement–admixture combinations with respect to the hydration process [29–37]. Therefore, it was used to investigate the effect of calcium sulfate on the hydration process in PC/CAC mixtures in this research. The study followed by other standard measurements, allowed to elucidate the scale of calcium sulfate utilization in PC/CAC mixtures, an important task from dry-mix mortars production point of view.

Experimental

The PC and CAC used in this study were obtained from Xinfra cement Co. and Kerneos cement Co, respectively. Three sources of calcium sulfate were used, natural anhydrite (A), gypsum (G), and α -hemihydrate (H). The chemical compositions of the raw materials used were determined by X-ray fluorescence (XRF), as shown in Table 1.

The binders were prepared with different sources and content of calcium sulfate, and the binder without calcium sulfate was set as a reference (Table 2). An isothermal heat-conduction calorimeter (TAM air C80, Thermometric, Sweden) was used to measure the hydration heat evolution of the binders. The water/binders ratio was 0.5 and the experimental temperature was 20 ± 0.1 °C. Binders and water were tempered for several hours before mixing, then the water was injected into the reaction vessel and the samples were stirred in the calorimeter for several minutes. This procedure allowed monitoring the heat evolution from the very beginning when water was added to the binders. Data logging was continued for about 7 days.

Setting time was determined by using a Vicat apparatus according to ISO 9597: 1989. Mortar samples (40 × 40 × 160 mm) for compressive strengths tests were prepared and measured according to ISO 679: 1989. These samples were demoulded after 24 h and randomly selected for mechanical testing after periods of 1, 3, and 28 days.

X-ray diffraction (XRD) was employed for detecting ettringite in cement pastes. Since the characteristic peak of ettringite is near about 9.1° , the scanning was performed between 8.5° and 9.5° with a 2θ increment 0.02° per min, step scanning mode, a dwell time of 4 s, and a Cu K α radiation. XRD data of ettringite were recorded using a Rigaku-D/max2550VB3+. The integrate area of ettringite was calculated automatically by the software of MDI Jade 5.0 with the function of “Profile fitting”. Before the test, the samples were ground to a fineness of about 400 m²/kg Blaine surface areas at the end of each aging period, treated

Table 2 Mix proportion of ternary system

Specimens no.	Mix proportion/g				
	P	T	A	G	H
S0	77.5	22.5	–	–	–
A1	77.5	15.0	7.5	–	–
A2	77.5	7.5	15.0	–	–
G1	77.5	15.0	–	7.5	–
G2	77.5	7.5	–	15.0	–
H1	77.5	15.0	–	–	7.5
H2	77.5	7.5	–	–	15.0

with acetone and diethyl-ether to stop hydration and stored in a desiccator to ensure protection against water and carbon dioxide.

Results and discussion

Calorimetric analysis

Without calcium sulfate

The rate of heat evolution for S0 illustrates a major difference from the curve of neat PC paste (Fig. 1). According to literatures [5], the first exothermic peak in the heat evolution curve of PC results from the complex reactions during the wetting process, and the second exothermic peak attributes to the C_3S and/or C_2S hydration. Compared with the curve of PC, there is a significant delay in the appearance of the second peak for the curve of S0. The so-called induction period associated with neat PC paste is about 2 h. However, it is much longer for S0. The maximum values of the rate for PC and S0 are 2.71 and $1.56 \text{ J (g h)}^{-1}$, and the corresponding time is 13.08 and 62.34 h. It means that the hydration of PC is significantly delayed with 22.5% CAC addition, which is consistent with the findings of Gu et al. [2, 29] and Gawlicki et al. [37]. This long dormant period could be explained by a surface coverage of the clinker grains by early hydration, which impeded further PC hydration [2, 29].

The total heat evolution curves for PC and S0 are illustrated in Fig. 2. The curve for S0 reveals two stages of heat evolution, one within first hours and another beyond 24 h, whereas the curve for the PC paste is continuous and does not appear to have such two distinct regions. In the first hydration stage of S0, the CAC in mixtures hydrates quickly and forms a thin layer on the surface of unhydrated

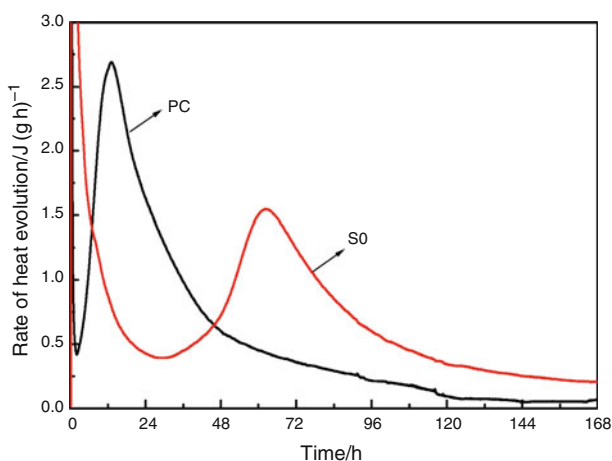


Fig. 1 Rate of heat evolution of the pure PC and S0 paste

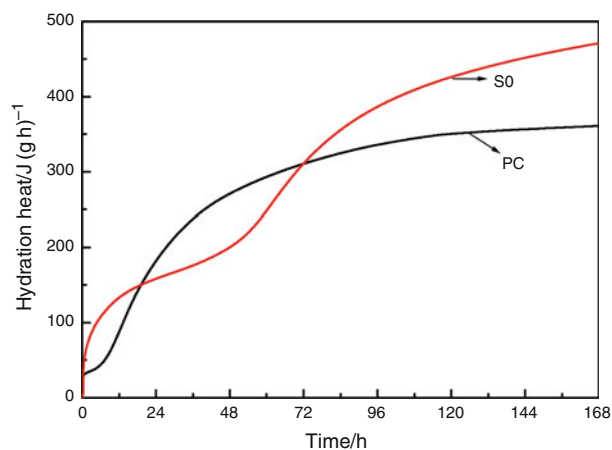


Fig. 2 Hydration heat of the pure PC and S0 paste

cement granules, and then after a long dormant period, the equilibrium is broke, and the second stage begins for the hydration of C_3S and C_2S in PC.

With low calcium sulfate addition

Figure 3 shows the rate of heat evolution of the ternary system with low calcium sulfate addition. Apart from the initial peak, there are three distinct exothermic peaks in the curves of A1 and H1. In addition, the second and third maximum rates of heat evolution of A1 are higher than that of H1. In contrast, there is only one distinct exothermic peak in the curve of G1 apart from the initial peak, which illustrates the formation of C–S–H gel and ettringite occurs simultaneously after wetting.

Plots of hydration heat of the ternary system with low calcium sulfate addition are given in Fig. 4. The paste with a low α -hemihydrate addition has the biggest cumulative heat release during the first several days, and reaches the

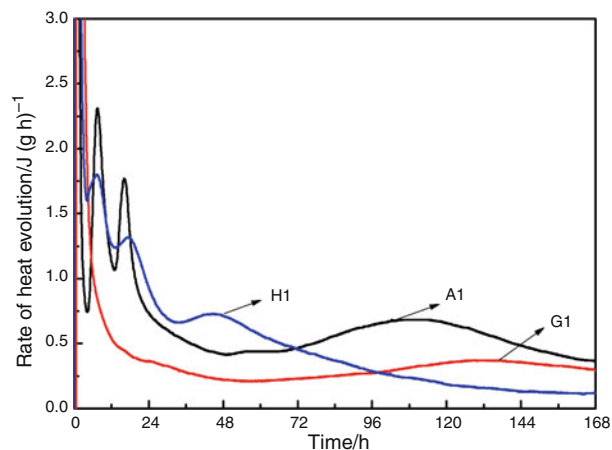


Fig. 3 Rate of heat evolution of the ternary system with low calcium sulfate addition

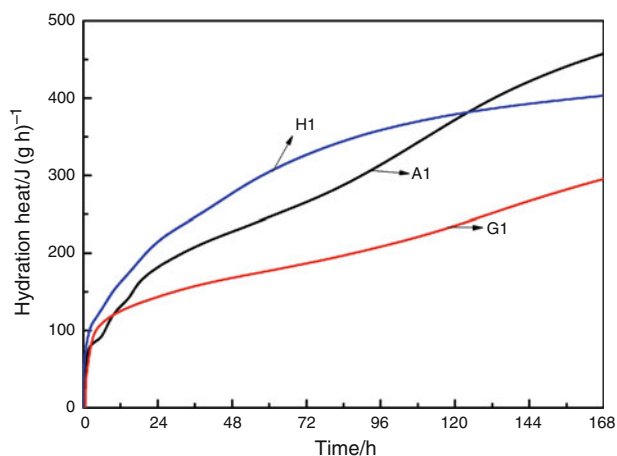


Fig. 4 Hydration heat of the ternary system with low calcium sulfate addition

cumulative heat release of 381 J (g h)^{-1} after 120 h hydration. However, the cumulative heat release for paste with insufficient anhydrite overpasses that with α -hemihydrate. Additionally, the paste with gypsum shows the smallest cumulative heat release except the first several hours.

With high calcium sulfate addition

All curves for samples with high calcium sulfate addition (Fig. 5) show a similar trend as PC and S0 (Fig. 1). However, the second exothermic peaks appear earlier than S0. It implies that calcium sulfate plays an accelerating role in the hydration of such ternary system. The maximum rates of heat evolution for G2, A2, H2 decline gradually, which are 2.51 , 2.10 , and $1.68 \text{ J (g h)}^{-1}$, respectively, and the corresponding time decreased in the following sequence $A2 > G2 > H2$.

Figure 6 shows the hydration heat of the ternary system with high calcium sulfate addition. The paste with gypsum

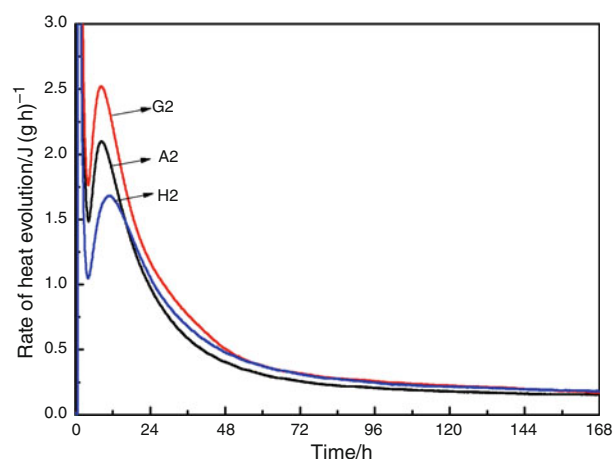


Fig. 5 Rate of heat evolution of the ternary system with high calcium sulfate addition

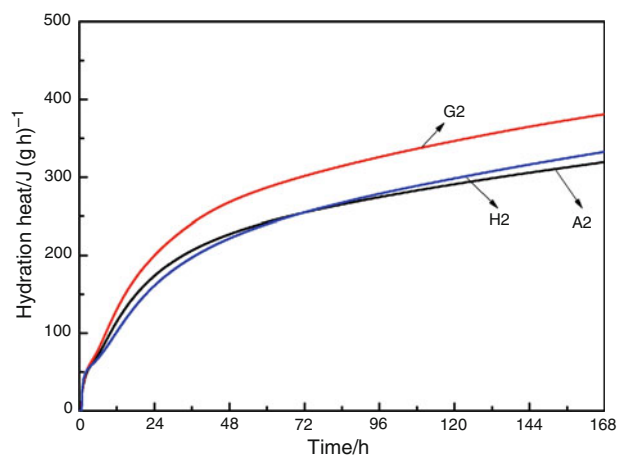


Fig. 6 Hydration heat of the ternary system with high calcium sulfate addition

has a higher hydration heat than the other pastes with anhydrite or α -hemihydrate. The cumulative heat release of three samples before 72 h increased in the following

Table 3 Setting time and compressive strength of mortars of ternary system

Specimens no.	Setting time/min		Compressive strength/MPa		
	Initial	Final	1 day	3 days	28 days
PC	195	278	21.4	31.7	44.2
S0	4	8	5.3	9.1	15.2
A1	14	24	11.9	23.8	31.2
A2	20	35	20.6	26.4	32.8
G1	6	15	15.2	25.3	27.6
G2	17	28	12.3	23.9	31.2
H1	8	16	17.1	30.3	37.4
H2	5	10	11.0	7.5	0

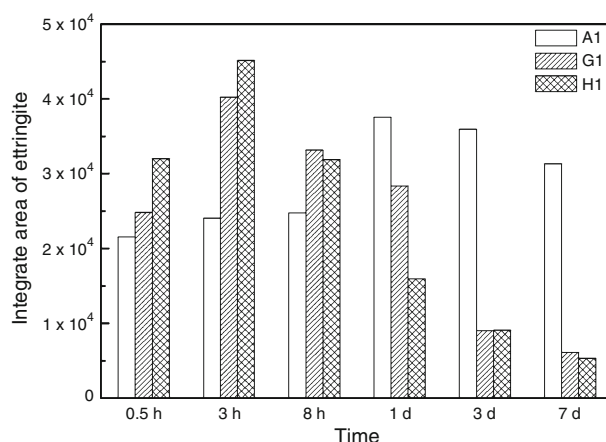


Fig. 7 Integrate area of ettringite in XRD patterns of A1, G1 and H1 at different curing times

Fig. 8 XRD patterns of A1 and H1 paste hydrated after 0.5 h, 8 h and 3 days: **a** A1 paste, **b** H1 paste

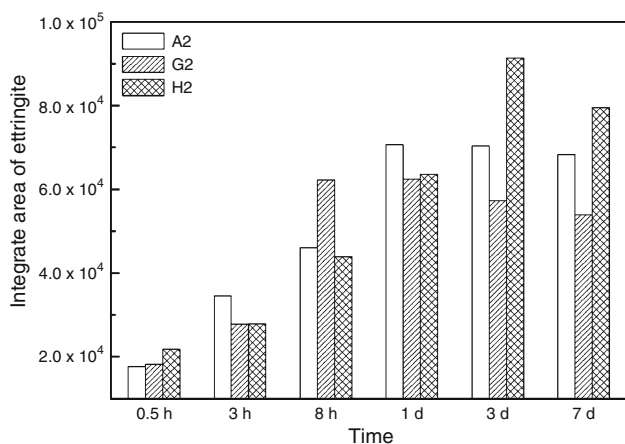
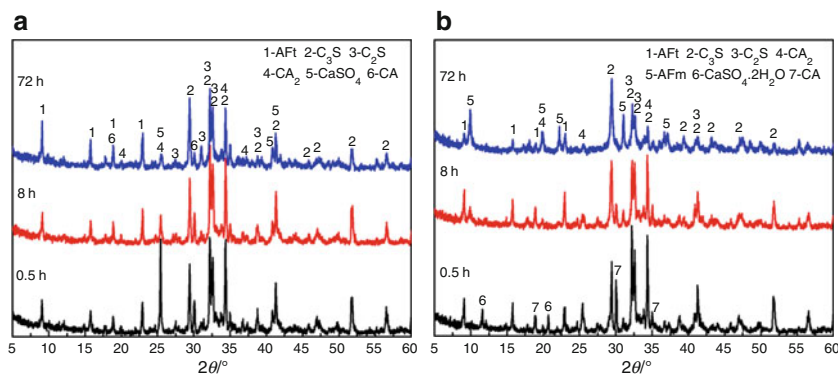


Fig. 9 Integrate area of ettringite in XRD patterns of A2, G2 and H2 at different curing times

sequence $G2 > A2 > H2$, but then the cumulative heat release of H2 catches up with that of A2.

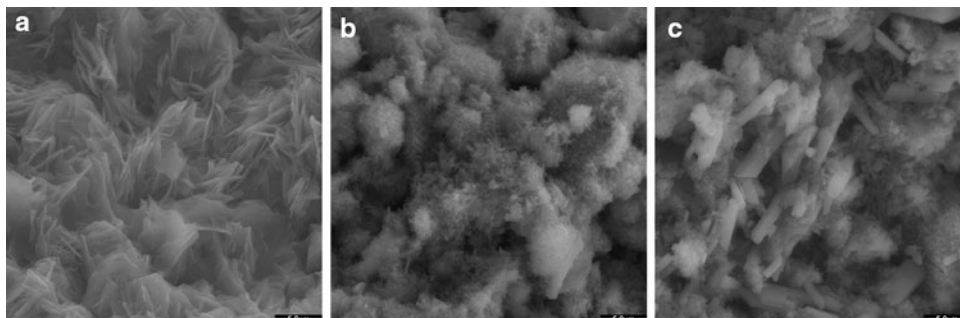
Setting time and physical strength

The setting time and compressive strength of mortars of the ternary system are shown in Table 3. For setting time test, in general, all the given mix proportion sets more quickly than the neat PC, but the ternary system has a longer setting time than the PC/CAC mixture (S0). It means that the

formation of ettringite retards setting when calcium sulfate is added. It is also observed that both initial and final setting time of the ternary system increase with increasing anhydrite and gypsum content, while both decrease with increasing α -hemihydrate addition. For instance, the paste with high α -hemihydrate (H2) addition has the shortest initial and final setting time of 5 and 10 min, respectively. It means that the microstructure of H2 paste develops quickly once in contact with water, which may result from the formation of secondary gypsum or ettringite.

As also can be seen in Table 3, compressive strength of all ternary system mortars is much higher than the control S0 mortar at the same curing time. Additionally, the compressive strength of mortars with high calcium sulfate addition is increased in the following sequence: $A1 < G1 < H1$ (except G1 mortar at 28 days) and $A2 > G2 > H2$. Furthermore, it is noticed that the compressive strength of H2 mortar is found to be lower than that of H1 mortar at all curing times (especially at 28 days), which results from the formation of large quantities of expansive gypsum and ettringite. The rates at which Ca^{2+} and SO_4^{2-} ions are supplied by the calcium sulfate thus depend both on the amount of the latter and on its physical and chemical nature. It is generally known that the dissolve rate of three sources of calcium sulfate is increased in the following sequence: hemi-hydrate $>$ gypsum $>$ anhydrite [22–24], which develop in an opposite trend with the compressive strength. The possible reason

Fig. 10 ESEM images of S0, A2 and H2 pastes after 1 day: **a** S0 paste, **b** A2 paste, **c** H2 paste



for this could be that large quantities of ettringite are formed within a short time, leading to a thin layer on unhydrated cement granules, which retains later strength development of the ternary system.

XRD and SEM analysis

Figure 7 shows integrate area of ettringite in XRD patterns of A1, G1, and H1 at different curing times. The content of ettringite in the three pastes first increases and then decreases: the content of ettringite in G1 and H1 pastes firstly reaches the maximum at 3 h and then decreases significantly, while that of A1 reaches the maximum at 1 day and then decreases slightly. This indicates that all the anhydrite, α -hemihydrate, and gypsum were consumed in the hydration reaction with calcium aluminate. Furthermore, the ettringite formed is most stable when anhydrite is added as a source of sulfate.

The XRD spectra of A1 and H1 pastes hydrated after 0.5 h, 8 h, and 3 days is shown in Fig. 8. As can be clearly seen from this figure, the characteristic peak of ettringite in the XRD spectra of A1 paste after hydrated for 0.5 h, 8 h, and 3 days grows continuously, while that in H1 paste firstly increases slightly and then decreases greatly, furthermore, the characteristic peak of monosulphoaluminate (AFm) in H1 paste grows obviously. It means that the first two peaks in Fig. 3 is concerning with the formation of ettringite and C–S–H gel, and the third one is associated with the transformation from ettringite to AFm. This result also confirms well with the great changes in the XRD analysis result of ettringite (Fig. 7) for different varieties of calcium sulfate used.

For those pastes with higher content of calcium sulfate, the integrate area of ettringite in XRD patterns of A2, G2, and H2 is shown in Fig. 9. On the one hand, the increase in sulfate content in mix proportion leads directly to obvious increase of ettringite formation content; on the other hand, since ettringite is less stable than AFm at ambient temperature, it tends to transform into AFm once the sulfate is depleted, and the transformation is more slightly than when a low content of calcium sulfate is added (Fig. 7).

The microstructure of S0, A2, and H2 pastes after 1 day of hydration was analyzed using ESEM as shown in Fig. 10a–c. It can be found that in the absence of calcium sulfate (Fig. 9a), the calcium aluminate hydrates (about 5 μm in size) develop in lamellar shape and are uniformly distribute in the voids between the cement particles, form bridges and thus causes rapid setting. Additionally, it can be seen that if a large amount of anhydrite is present (Fig. 10b), corresponding ettringite (about 0.5–1 μm in size) forms directly on the surface of cement particles, but not between the voids. By comparing Fig. 10b with Fig. 10c, if large amount of α -hemihydrate is added

(Fig. 10c), ettringite and coarser needle-like secondary gypsum (also about 5 μm in size) forms in the voids, causing rapid setting. In general, the meshwork of plates, are in contrasted with the much more compact coatings of gel and small rods of the ettringite phase formed in the presence of an adequate supply of gypsum [5].

Conclusions

Based on the experimental results, it could be concluded that the source and amount of calcium aluminate play a key role in the hydration of PC/CAC mixtures, and especially affect the formation of ettringite.

1. Calorimetry shows that without calcium aluminate addition, the second exothermic peak appears almost 50 h later than that of neat PC, which indicates that the hydration of PC is significantly delayed by CAC; with calcium aluminate addition, a high amount of ettringite forms within the hardened matrix and shows an obvious exothermic peak in the curves of rate of heat evolution.
2. The decrease in ettringite results from the transformation from ettringite to AFm due to the shortage of sulfate in the pore solution. If anhydrite is added as a source of sulfate, the ettringite formed is comparatively most stable.
3. When calcium sulfate is added, the setting time is prolonged and the compressive strength of PC/CAC mixtures mortars at all curing ages is also improved, especially with a high content of anhydrite or a low content of α -hemihydrate.
4. In the absence of calcium sulfate, the calcium aluminate hydrates develop in lamellar shape and distribute uniformly in the voids between the cement particles; but ettringite forms directly on the surface of cement particles if a large amount of anhydrite is present, moreover, ettringite and coarser needle-like secondary gypsum forms in the voids when a large amount of α -hemihydrate is added.

Acknowledgements The authors acknowledge greatly the financial support of this work by the fund of National Key Technology R&D Programs in the 11th Five-year Plan of China (2006BAJ05B03).

References

1. Wu ZB, Guan BH, Lou WB, Ye QQ, Fu HL. Calorimetric study of calcium aluminate cement blended with flue gas desulfurization gypsum. *J Therm Anal Calorim.* 2009;98(3):737–42. doi: 10.1007/s10973-009-0107-3.
2. Gu P, Beaudoin JJ, Quinn EG, Myers RE. Early strength development and hydration of ordinary Portland cement calcium aluminate cement pastes. *Adv Cem Res.* 1997;6(2):53–8.

3. Amathieu L, Bier A, Scrivener K. Mechanisms of set acceleration of Portland cement through CAC addition. In: International Conference on Calcium Aluminate Cement, Edinburgh; 2001.
4. Gu P, Fu Y, Xie P, Beaudoin JJ. A study of the hydration and setting behavior of OPC-HAC pastes. *Cem Concr Res.* 1994; 24(4):682–94.
5. Taylor HFW. *Cement chemistry*. 2nd ed. London: Thomas Telford; 1997.
6. Zhang X, Yang Y, Ong CK. Study of early hydration of OPC-HAC blends by microwave and calorimetry technique. *Cem Concr Res.* 1997;27(9):1419–28.
7. Garces P, Alcocel EG, Andreau CG. Hydration characteristics of high alumina cement-Portland cement mixtures. *Zkg Int.* 1998;51(11):646–9.
8. Osborne GJ, Breccem A. Rapid hardening cement-based on high alumina cement. *Proc ICE Struct B.* 1994;104(1):93–100.
9. Majumdar AJ, Singh B, Edmonds RN. Hydration of mixtures of cement-Fondu aluminous cement and granulated blast furnace slag. *Cem Concr Res.* 1990;20(2):197–208.
10. Gu P, Beaudoin JJ. Effect of lithium salts on Portland cement-high alumina cement paste hydration. *J Mater Sci Lett.* 1995;14(17):1207–9.
11. Gu P, Beaudoin JJ. Lithium salt-based additives for early strength-enhancement of ordinary Portland cement-high alumina cement paste. *J Mater Sci Lett.* 1997;16(9):696–8.
12. Hirano Y, Makida K, Komatsu R, Ikeda K. Dimensional change of self-leveling materials developed by mixing aluminous cement, Portland cement and anhydrite at 35 degrees C. *Trans Mater Res Soc Jpn.* 2006;31(2):325–8.
13. Seifert S, Neubauer J, Goetz-Neunhoeffler F, Motzet H. Application of two-dimensional XRD for the characterization of the microstructure of self-leveling compounds. *Powder Diffr.* 2009;24(2):107–11. doi:10.1154/1.3132642.
14. Bier TA, Nukita M. Influence of redispersible powder on expansion in self leveling underlayments. In: Proceedings of the 6th Asian Symposium on Polymers in Concrete. 2009. p. 222–7.
15. Onishi K, Bier TA. Investigation into relations among technological properties, hydration kinetics and early age hydration of self-leveling underlayments. *Cem Concr Res.* 2010;40(7):1034–40. doi:10.1016/j.cemconres.2010.03.004.
16. De Gasparo A, Herwegh M, Zurbriggen R, Scrivener K. Quantitative distribution patterns of additives in self-leveling flooring compounds (underlayments) as function of application, formulation and climatic conditions. *Cem Concr Res.* 2009;39(4):313–23. doi:10.1016/j.cemconres.2008.12.009.
17. Sang GC, Liu JP. Study of properties of Portland and aluminate cementitious composited grouting material. *Mater Res Innov.* 2010;14(3):200–5. doi:10.1179/143307510x12719005364387.
18. Sakai E, Nikaido Y, Itoh T, Daimon M. Ettringite formation and microstructure of rapid hardening cement. *Cem Concr Res.* 2004;34(9):1669–73.
19. Kighelman J, Scrivener K, Zurbriggen R, editors. Effect of the mix binder system on the hydration of self-leveling compounds. 16th international conference on building materials; 2006; Weimar.
20. Weyer HJ, Muller I, Schmitt B, Bosbach D, Putnis A. Time-resolved monitoring of cement hydration: influence of cellulose ethers on hydration kinetics. *Nucl Instrum Methods B.* 2005;238(4):102–6. doi:10.1016/j.nimb.2005.06.026.
21. Odler I, Colan-Subauste J. Investigations on cement expansion associated with ettringite formation. *Cem Concr Res.* 1999;29(5): 731–5.
22. Meifei S, Zhongyan D, Kezong L. Effects of different forms of calcium sulfate on the hydration and properties of casting cement. *J Chin Silic Soc.* 1982;10(3):298–310.
23. Xiuji F, hui W. The influence of gypsum on some properties of sulphoaluminate high early strength cement. *J Chin Silic Soc.* 1984;12(2):166–78.
24. Zhang H, Odler I. Investigations on high SO₃ portland clinkers and cements—properties of cements. *Cem Concr Res.* 1996; 26(9):1315–24.
25. Evju C, Hansen S. The kinetics of ettringite formation and dilatation in a blended cement with beta-hemihydrate and anhydrite as calcium sulfate. *Cem Concr Res.* 2005;35(12):2310–21. doi: 10.1016/j.cemconres.2004.09.012.
26. Pourchet S, Regnaud L, Perez JP, Nonat A. Early C₃A hydration in the presence of different kinds of calcium sulfate. *Cem Concr Res.* 2009;39(11):989–96. doi:10.1016/j.cemconres.2009.07.019.
27. Puri A, Voicu G, Badanoiu A. Expansive binders in the Portland cement-calcium aluminate cement- calcium sulfate system. *Rev Chim-Bucharest.* 2010;61(8):740–4.
28. Bensted J, Barnes P. *Structure and performance of cements*. 2nd ed. London: Taylor & Francis group; 2008.
29. Gu P, Beaudoin JJ. A conduction calorimetric study of early hydration of ordinary Portland cement high alumina cement pastes. *J Mater Sci.* 1997;32(14):3875–81.
30. Sauvat N, Sell R, Mougel E, Zoulalian A. A study of ordinary portland cement hydration with wood by isothermal calorimetry. *Holzforschung.* 1999;53(1):104–8.
31. Sha W. Differential scanning calorimetry study of the hydration products in Portland cement pastes with metakaolin replacement. In: Proceedings of the International Conference on Advances in Building Technology, Vols. I, II. 2002. p. 881–8.
32. Evju C. Initial hydration of cementitious systems using a simple isothermal calorimeter and dynamic correction. *J Therm Anal Calorim.* 2003;71(3):829–40.
33. Pane I, Hansen W. Investigation of blended cement hydration by isothermal calorimetry and thermal analysis. *Cem Concr Res.* 2005;35(6):1155–64. doi:10.1016/j.cemconres.2004.10.027.
34. Pacewska B, Wilinska I, Blonkowski G. Investigations of cement early hydration in the presence of chemically activated fly ash—use of calorimetry and infrared absorption methods. *J Therm Anal Calorim.* 2008;93(3):769–76. doi:10.1007/s10973-008-9143-7.
35. Ylmen R, Wadso L, Panas I. Insights into early hydration of Portland limestone cement from infrared spectroscopy and isothermal calorimetry. *Cem Concr Res.* 2010;40(10):1541–6. doi: 10.1016/j.cemconres.2010.06.008.
36. Gruyaert E, Robeyst N, De Belie N. Study of the hydration of Portland cement blended with blast-furnace slag by calorimetry and thermogravimetry. *J Therm Anal Calorim.* 2010;102(3): 941–51. doi:10.1007/s10973-010-0841-6.
37. Gawlicki M, Nocun-Wczelik W, Bak L. Calorimetry in the studies of cement hydration. *J Therm Anal Calorim.* 2010;100(2): 571–6. doi:10.1007/s10973-009-0158-5.